Charge Recombination Dynamics of Geminate Ion Pairs Formed by Electron Transfer Quenching of Molecules in an Upper Excited State

Pierre-Alain Muller and Eric Vauthey*

Institut de Chimie-Physique de l'Université de Fribourg, Pérolles, CH-1700 Fribourg, Switzerland

Received: January 4, 2001; In Final Form: April 6, 2001

An investigation of the charge recombination (CR) dynamics of geminate ion pairs formed upon electron transfer quenching of azulene, benz[*a*]azulene, and xanthione in the second singlet excited state by several electron donors, using ultrafast time resolved spectroscopy and photoconductivity is reported. The ion pairs have two possible CR pathways: (i) a highly exergonic CR to the neutral ground state or (ii) a moderately exergonic CR leading to the formation of the neutral acceptor in the first singlet excited state. This investigation shows strong evidence of the predominance of the second pathway. CR in ion pairs formed with the azulenes is faster by a factor of more than 50 than in ion pairs having a similar energy but with the first CR pathway only. The electron transfer quenching of xanthione in the second singlet excited state by several weak donors does not lead to a significant reduction of the triplet yield of this molecule. The relevance of these results to explain the absence of the inverted region in highly exergonic bimolecular charge separation reactions is discussed.

Introduction

One of the remaining problems in bimolecular photoinduced electron transfer (ET) reactions is the absence of inverted region, predicted by the Marcus theory,[1] in the high exergonicity regime.[2] This behavior can be explained to a large extent by an increase of the ET distance with increasing free energy. This idea has been developed in the Tachiya−Murata model, which can reproduce the free energy dependence of the ET quenching rate constants measured by Rehm and Weller.[3] However, it appears that to account for the lack of inverted region for very exothermic ET ($\Delta G < -2$ eV) unrealistically large values of the electronic coupling matrix element have to be invoked.[4] It has been proposed that, for these processes, the product could be formed in an electronic excited state. If this is the case, the reaction is no longer highly exergonic and thus does not take place in the inverted regime. The product molecules of charge separation (CS) reactions are open-shell radical ions, which are known to have low energy electronic excited states.[5] However, the formation of excited radical ions in highly exothermic CS has never been observed so far. Excited radical ions are difficult to detect in the condensed phase; there are indeed very few reports on fluorescence from excited open-shell ions in liquids.[6−9] This is due to fast nonradiative transitions, favored by a small D_1-D_0 energy gap.[10] Moreover, the radical ions of most compounds used in ET quenching experiments have a weak oscillator strength for the $D_1 \leftarrow D_0$ transition and therefore a small radiative rate constant.

The situation is apparently more favorable for the charge recombination (CR) reaction of radical ions, where the product molecules are closed shell species. For example, the phenomenon of electrogenerated chemiluminescence is due to the homogeneous recombination of high energy radical ions, formed electrochemically, to an electronic excited state of one of the product molecules.[11] With most organic systems, the homogeneous ionic recombination leads predominantly to the low lying triplet excited state, which can then populate the excited singlet state via triplet−triplet annihilation.[12] The preferential triplet state population is not only due to the lower energy of this state but also to the spin statistics related to the homogeneous recombination of radical ions. The situation is different for geminate recombination, where the spin correlation of the ions has not been lost. In this case, the CR dynamics strongly depends on the spin multiplicity of the GIP.[13] We have recently investigated the dynamics of CR in triplet geminate ion pairs (GIPs) with electron acceptor/donor (A/D) pairs, where D had a low lying triplet excited state.[14] In this case, there were two CR pathways: (i) a moderately to highly exergonic and spin-forbidden CR to the neutral ground state, A + D, and (ii) a weakly exergonic and spin-allowed CR leading to the formation of the neutral donor in the triplet state, A + D*(T_1). It was shown that geminate CR was only taking place via the second pathway.[14] In this system, however, the branching between these pathways is not controlled by their relative exergonicity but only by spin conservation. It is indeed known that spin-forbidden CR take place in the sub-microsecond time scale,[15] while spin-allowed CR can occur in the subpicosecond time scale.[16]

We report here on the investigation of the dynamics of singlet GIPs that also have two possible CR pathways: (i) a highly exergonic CR to the neutral ground state, A + D and (ii) a moderately exergonic CR leading to the neutral acceptor in the first singlet excited state, A*(S_1) + D. Contrary to the above-mentioned case, both pathways are spin allowed, and the competition between them should mainly be controlled by their relative exergonicity.

These GIPs are formed by ET quenching of azulene (AZ), benz[*a*]azulene (BZ) and xanthione (XA) in the second singlet excited state, S_2, by various electron donors in acetonitrile. The structure of these compounds is shown in Charts 1 and 2 together with their excited-state energy and redox potential. We will present evidence for the predominance of the second CR

* Corresponding author; new address: Dept. de Chimie Physique de l'Université de Genève, 30 quai Ernest Ansermet, CH-1211 Genève 4, Switzerland. E-mail: eric.vauthey@chiphy.unige.ch.

10.1021/jp010015z CCC: $20.00
Published on Web 06/05/2001

CHART 1. Electron Acceptors (Reduction Potentials vs SCE)

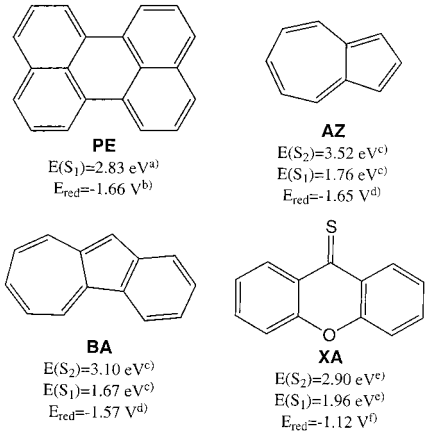

[a] Ref 17. [b] Ref 18. [c] Ref 19. [d] Ref 20. [e] Ref 21. [f] In 0.1 M tetrabutylammonium hexafluorophosphate in ACN.

CHART 2. Electron Donor (Oxidation Potentials vs SCE)

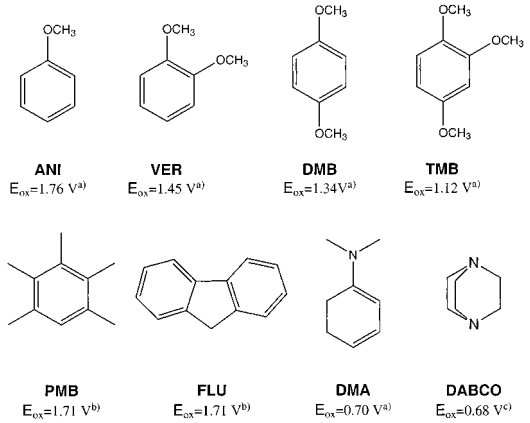

[a] Ref 22. [b] Ref 23. [c] Ref 24.

pathway. The relevance of these results to explain the absence of inverted region in CS will also be discussed.

Experimental Section

Ultrafast Spectroscopy. the ET quenching dynamics of BA and XA in the S_2 state has been measured using the multiplex transient grating (TG) technique.[25] The TG setup has been described in details elsewhere.[26] Briefly, excitation was performed by two time coincident laser pulses around 400 nm, crossing the sample with an angle of 1.2°. These pulses were obtained by frequency doubling the output of a standard 1 kHz amplified Ti:Sapphire system (Spectra-Physics). The duration of the pulses was about 120 fs, and the pump energy on the sample was around 20 μJ with a spot-size of 1.5 mm diameter.

About 10% of the unconverted output at 800 nm were sent along an optical delay line before being focused in a 10-mm quartz cell filled with a 70/30 (V/V) D_2O/H_2O mixture for supercontinuum generation. The resulting white light pulses were then recollimated and then focused on the sample to a spot of about 0.75 mm diameter with an angle of incidence of 0.8°. The polarization of the pump pulses was oriented at magic angle relative to that of the probe pulses. The diffracted signal was passed through a cutoff filter (Schott CG 430) to eliminate scattered pump light and was then focused with a combination of spherical and cylindrical lenses on the entrance of a 1/4 m imaging spectrograph (Oriel Multispec 257) equipped with a 1024×256 pixels air cooled CCD camera (Oriel Instaspec IV). All TG spectra were corrected for the chirp of the white light pulses.

The quenching dynamics of AZ in the S_2 state has been monitored by transient absorption (TA) spectroscopy. Excitation was performed at 355 nm with the third harmonic output of a passive/active mode-locked Nd:YAG laser (Continuum PY61-10). The pulse duration was around 25 ps, the repetition rate was 10 Hz, and the pump intensity on the sample was around 10 mJ/cm^2. The transmission was probed either at 532 nm with the second harmonic output of the laser or at 630 nm by Raman shifting the 532 nm pulses in ethanol.

Free Ion Yield Measurements. The free ion yields have been determined using photoconductivity (PC).[27] The photocurrent cell has been described in detail previously.[28] The samples were excited at 355 nm using the frequency tripled output of a Q-switched Nd:YAG laser (Continuum Surelite II-10). The pulse energy was 8 mJ, and the duration was 6 ns. The system benzophenone with 0.02 M 1,4-diazabicy-clo[2.2.2]octane in acetonitrile, which as a free ion yield of unity, was used as a standard.[29]

Low-Temperature Spectra of Free Radical Anions. To measure the electronic spectra of radical anions, frozen solutions ($T = 77$ K) of the neutral molecules in methyl-tetrahydrofuran have been exposed to γ-irradiation from a ^{60}Co source (Gammacell 220 MDS Nordion Inc).[30]

Samples. Azulene (AZ), perylene (PE), pentamethylbenzene (PMB), fluorene (FLU), and 1,4-dimethoxybenzene (DMB) were recrystallized. Anisol (ANI), Veratrol (VER), 1,2,4-trimethoxybenzene (TMB), and *N*,*N*-dimethylaniline (DMA) were distilled, while 1,4-diazabicyclo[2.2.2]octane (DABCO) was sublimed. Acetonitrile (ACN, Fluka UV grade) was used without further purification. Benz[*a*]azulene was given by Prof. E. Haselbach from the University of Fribourg and was purified by column chromatography. Xanthione (XA) was synthesized according to the literature[31] and purified by column chromatography and sublimation. Unless specified all compounds were from Fluka.

For TG measurements, the sample solutions were placed in a 1-mm cell and the absorbance at 400 nm was around 0.4, corresponding to concentrations of 10^{-3} M and 2.5×10^{-4} M for BA and XA, respectively. For TA, a 1-cm cell was used, and the concentrations were 2.5×10^{-4} M and 10^{-3} M for PE and AZ, respectively, corresponding to an absorbance of 1 at 355 nm. During the measurements, the samples were continuously stirred by N_2 bubbling. For PC measurements, the concentrations were 1.2×10^{-4} M for PE, 5×10^{-4} M for AZ, 1.3×10^{-4} M for BA and 1.2×10^{-4} M for XA. These concentrations result in an absorbance at 355 nm of 0.5 on 1 cm. No significant sample degradation was observed after the measurements. All experiments were performed at 20 ± 1 °C.

Results and Discussion

(A) Comparison of the CR in AZ$^{\bullet-}$/D$^{\bullet+}$ and PE$^{\bullet-}$/D$^{\bullet+}$ Pairs. In a first stage, we have compared the CR dynamics of GIP formed by ET quenching of AZ in the S_2 state and PE in the S_1 state by various electron donors. The free energy for the initial CS can be calculated as $\Delta G_{CS} = E_{ox}(D) - E_{red}(A) - E(S_2)$,[32] where $E_{ox}(D)$ and E_{red} (A) are the oxidation and reduction potential of D and A, respectively, and where the electrostatic interaction energy between the ions is neglected. Similarly the free energy of CR to the neutral ground state is given by $\Delta G_{CR} = E_{red}$ (A) $- E_{ox}(D)$. As AZ and PE have almost identical reduction potentials, ΔG_{CR} is very similar for AZ$^{\bullet-}$/

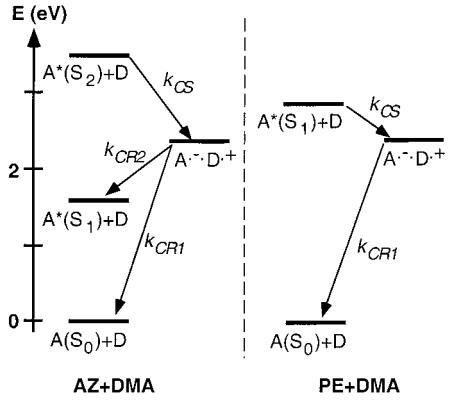

Figure 1. Energy diagrams of the states involved in the photoinduced ET reaction of AZ and PE with DMA.

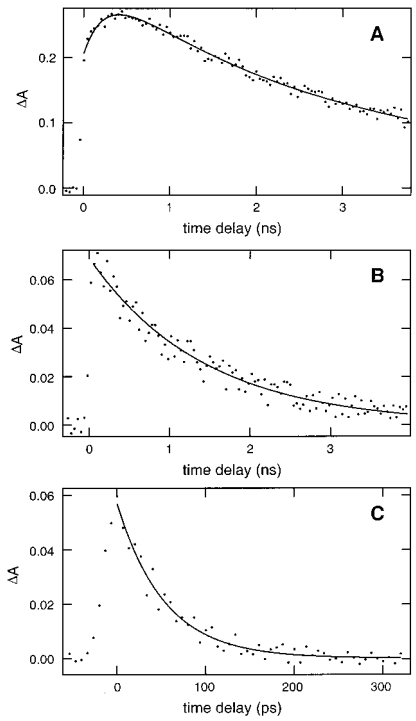

Figure 2. Time profiles of the transient absorption at 532 nm after excitation at 355 nm of solutions of (A) PE + 0.5 M TMB, (B) AZ, and (C) AZ + 0.55 M TMB in ACN and best fits (solid lines).

$D^{\bullet+}$ and $PE^{\bullet-}/D^{\bullet+}$ pairs when the donor is the same, as shown in Figure 1. For $AZ^{\bullet-}/D^{\bullet+}$ pairs however, there is a second CR pathway to $AZ^*(S_1)/D$ with a free energy $\Delta G_{CR}^* = E_{red}(A) - E_{ox}(D) + E(S_1)$.

Figure 2A shows the time profile of the transient absorbance at 532 nm measured with a solution of PE with 0.5 M TMB in ACN. The initial rise of the absorbance is due to the built up of the $PE^{\bullet-}$ population, whose absorption maximum is around 570 nm,[33] upon ET quenching of $PE^*(S_1)$. The latter also absorbs at 532 nm and is responsible for the signal intensity at time zero. The triplet yield of PE being inferior to 0.01,[34] this state is not involved in the ET quenching process. The time window of the experiment is too narrow to see the complete disappearance of the transient signal, but this profile can be well reproduced with a double exponential function, accounting for the formation and the decay of $PE^{\bullet-}$ population. The transient absorption decays to a constant value different from zero. This decay corresponds to the disappearance of $PE^{\bullet-}$ in the GIP by both CR to the ground state and dissociation to free ions. The remaining absorbance, which is constant on this time scale, is due to the free $PE^{\bullet-}$ population, which decays on a microsecond time scale by homogeneous recombination.[35] A qualitatively similar time profile has been measured with DMA as the donor.

TABLE 1: Separation Efficiency, Φ_{sep}, (error on Φ_{sep}: ±0.02) and Rate Constant of CR Measured for the GIPs Formed by ET Quenching of PE and AZ by Various Electron Donors

A/D	ΔG_{CR} (eV)	Φ_{sep}	k_{CR} (ns^{-1})
PE/TMB	−2.78	0.20	0.37
PE/DMA	−2.36	0.67	0.25
AZ/FLU (0.3 M)	−3.36	0.02	>3
AZ/PMB (0.3 M)	−3.36	0.03	>5
AZ/VER (0.55 M)	−3.10	<0.03	>15
AZ/TMB (0.55 M)	−2.77	0.02	>20
AZ/DMA (0.55 M)	−2.35	<0.03	>17

Assuming that the quenching of PE involves the formation of one type of GIP only, namely, the loose or solvent separated ion pair, the rate constants of CR, k_{CR}, and the rate constant of separation to free ions, k_{sep} can be extracted from the measured rate constant of GIP population decay, k_{GIP}:

$$\Phi_{ion} = \Phi_q \cdot \Phi_{sep} = \Phi_q \cdot \frac{k_{sep}}{k_{sep} + k_{CR}} \qquad (1)$$

where Φ_{ion} is the free ion yield, Φ_q is the quenching efficiency and Φ_{sep} is the separation efficiency. Given the relatively long lifetime of $PE^*(S_1)$[34] and the high donor concentration used, Φ_q is close to unity. The separation efficiencies, as well as the k_{CR} values calculated from eq 1 are listed in Table 1.

Figure 2B shows the time profile of the transient absorbance measured at 532 nm after excitation at 355 nm of a solution of AZ in ACN. The signal decays exponentially to zero with a time constant of 1.3 ± 0.1 ns. This transient can be ascribed to $AZ^*(S_2)$, because the absorption spectrum of this state is known to exhibit a broad band with a maximum near 530 nm[36] and because the S_2 fluorescence lifetime of AZ has been reported to be around 1.3 ns.[37]

Figure 2C shows the transient absorbance at 532 nm measured with a solution of AZ and 0.55 M TMB. The transient decays to zero with a time constant of 50 ± 10 ps. There can be two different contributions to this signal: $AZ^*(S_2)$ and azulene radical anion, $AZ^{\bullet-}$, whose absorption spectrum exhibits a band with a maximum at 440 nm and a shoulder around 530 nm.[33] However, we ascribe this signal to the $AZ^*(S_2)$ for the following reasons:

(i) The measured decay time depends on the concentration of TMB. It becomes shorter as the concentration of TMB increases as expected for dynamic quenching.

(ii) As compared to the S_2 lifetime of 1.3 ns, the lifetime of 50 ps observed with 0.55 M TMB corresponds to a quenching efficiency of about 0.96, in accordance with steady-state fluorescence measurements.

(iii) The initial signal intensity at 532 nm is similar for AZ alone and for AZ/TMB.

The fact that the contribution of $AZ^{\bullet-}$ is not observed can be explained by a rate constant of CR much faster than the quenching rate constant. The PC measurements confirm this hypothesis, as the free ion yield at 0.55 TMB, hence Φ_{sep}, is inferior to 0.03. This indicates that CR of the GIP is much faster than separation to free ions. Finally, the involvement of $AZ^*(T_1)$ can be ruled out, as the efficiency of both $S_2 \rightarrow T_1$ and $S_1 \rightarrow T_1$ intersystem crossings is smaller than 0.01.[38,39]

Similar measurements at 532 nm have been repeated with VER, DMA, PMB, and FLU as quenchers. The results are qualitatively the same as with TMB, namely, the signal decays

exponentially to zero with a time constant decreasing with increasing quencher concentration. The decay constants obtained at the highest quencher concentration are listed in Table 1. No contribution from the radical ions could be observed. The radical cation $PMB^{\bullet+}$ is known to absorb at 532 nm,[40] and thus the presence of a $PMB^{\bullet+}$ population with a lifetime larger than 200 ps would have certainly not been missed. Similarly, the system AZ/FLU has been probed at 630 nm in the absorption band of $FLU^{\bullet+}$,[33] and no transient absorption signal has been observed. The free ion yield with all these donors is extremely small, confirming the occurrence of a very fast CR.

If one compares AZ/DMA with PE/DMA or AZ/TMB with PE/TMB, it is immediately clear that CR with $AZ^{\bullet-}$ is much faster than with $PE^{\bullet-}$, although the reaction free energies are very similar. The ratio of the rate constants $k_{CR}(AZ^{\bullet-})/k_{CR}(PE^{\bullet-})$ is larger than 50 for both TMB and DMA! Apart from free energy, the ET rate constant also depends on the intramolecular and solvent reorganization energies, λ_i and λ_s, and on the electronic coupling matrix element, V.[1] AZ and PE are both aromatic hydrocarbons, and therefore the intramolecular reorganization energy upon reduction must be similar in both cases. According to the dielectric continuum theory, λ_s depends on the radius of the ions and on their center-to-center distance. AZ is substantially smaller than PE, and therefore, the solvent reorganization energy should be smaller for CR in $PE^{\bullet-}/D^{\bullet+}$ pairs. The molecular volumes of AZ and PE, calculated using the van der Waals increment method are 123 and 225 Å^3, respectively.[41] Assuming spherical shapes for the reactant molecules and contact distance for CR, λ_s in ACN should be larger for $AZ^{\bullet-}/D^{\bullet+}$ than for $PE^{\bullet-}/D^{\bullet+}$ pairs by about 0.1 eV. As CR to the neutral ground state should occur in the inverted regime ($\Delta G_{CR}(PE^{\bullet-}/DMA^{\bullet+}) = -2.36$ eV), an increase of λ_s at constant ΔG_{CR} should lead to an increase of the CR rate constant. Considering the free energy dependence of CR reported for this type of GIP,[16,26,35] this increase should not be larger than a factor 2−3, i.e., much smaller than that observed. The electron coupling matrix element V can be expected to be smaller for $PE^{\bullet-}/D^{\bullet+}$ than for $AZ^{\bullet-}/D^{\bullet+}$ pairs. Indeed, V is related to the overlap integral of the reactants wave functions. The charge being more localized in $AZ^{\bullet-}$ than in $PE^{\bullet-}$, the wave functions involved in the CR can be expected to be less diffuse in the $AZ^{\bullet-}/D^{\bullet+}$ than in the $PE^{\bullet-}/D^{\bullet+}$ pairs. Such a charge dilution effect has been recently invoked to account partially for the influence of steric hindrance on CR dynamics of GIPs.[42] It is, however, doubtful that a variation of V could account for the remaining difference of CR rate constants. Indeed, $V(AZ^{\bullet-}/D^{\bullet+})$ should be more than five times larger than $V(PE^{\bullet-}/D^{\bullet+})$! According to indirect measurements of k_{CR} in GIPs formed by ET quenching of cyanoanthracene derivatives by electron donors of various size, V increases by a factor 1.4 by going from phenanthrene derivatives (three-ring donors) to benzene derivatives (one-ring donors).[23] Therefore, these results strongly suggest that the primary product of CR with the $AZ^{\bullet-}/D^{\bullet+}$ GIPs is the excited product $AZ^*(S_1) + D$. In this case, the effective free energy for CR is $\Delta G_{CR}^* = \Delta G_{CR} + E(AZ^*(S_1))$, and the recombination is no longer deep in the inverted region but rather close to the barrierless region ($-\Delta G_{CR} \approx \lambda_i + \lambda_s$). In this free energy region, k_{CR} as fast as 10^{12} s^{-1} have been measured.[26] An unambiguous proof of this CR pathway would be the observation of the formation of $AZ^*(S_1)$ after ET quenching of $AZ^*(S_2)$. However, the lifetime of $AZ^*(S_1)$ is very short and depends on the degree of vibrational excitation: it varies from 1.7 ps, when not vibrationally excited, to 400 fs, when excited with 1300 cm^{-1} excess energy.[43] This lifetime is much shorter than the quenching time of $AZ^*(S_2)$, and thus this state cannot be observed.

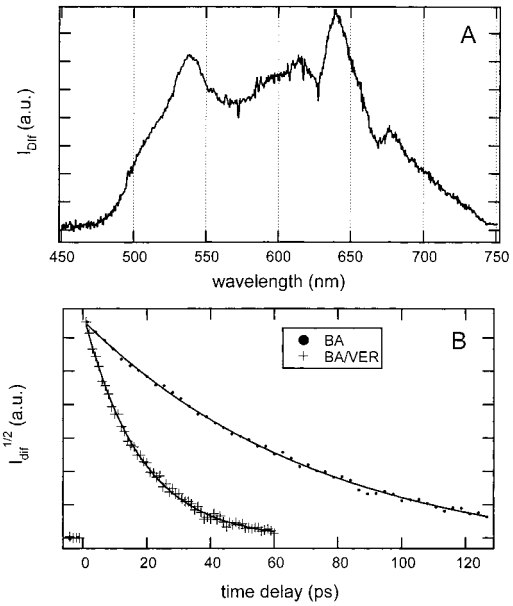

Figure 3. (A) Transient grating spectrum obtained 15 ps after excitation at 400 nm of a solution of BA in ACN; (B) time profiles of the square root of the diffracted intensity at 538 nm measured with BA and with BA + 1 M VER in ACN and best single-exponential fits (solid lines).

TABLE 2: Decay Time of $BA^*(S_2)$, τ_{S2}, with Various Electron Donors in ACN

A/D	ΔG_{ET}	ΔG_{CR}	τ_{S2} (ps)
BA alone			74
BA/VER (0.5 M)	−0.08	−3.02	54
BA/VER (1 M)	−0.08	−3.02	16
BA/DMA (0.5 M)	−0.83	−2.27	17
BA/DMA (1 M)	−0.83	−2.27	14

(B) $BA^{\bullet-}/D^{\bullet+}$ Pairs. Figure 3A shows the TG spectrum measured 15 ps after excitation of a solution of BA in ACN. The nature of a TG spectrum has been discussed in detail elsewhere.[25,44] In brief, the signal intensity is proportional to the square of the photoinduced changes of absorbance and refractive index. Therefore, the TG spectrum is the sum of the squares of the TA and of the transient dispersion spectra. The spectral features of a TG spectrum are dominated by the absorption spectrum, the band maxima being at the same position as in a TA spectrum. The major advantage of multiplex TG over TA is the superior sensitivity of the former technique, due to its zero background nature. In summary, a TG spectrum is very similar to a TA spectrum, and the TG intensity is proportional to the square of transient concentration. Figure 3B shows the time evolution of the square root of the TG intensity, which is proportional to the transient concentration, at 538 nm. The signal decays exponentially to zero with a time constant of 74 ps. BA is known to exhibit S_2-S_0 fluorescence like AZ, but with a substantially weaker quantum yield.[19,45] Consequently, this transient is ascribed to $BA^*(S_2)$.

The same measurements have been repeated with BA solutions containing high concentrations of electron donor (VER and DMA). The resulting TG spectra are the same as those observed without quencher, but their lifetimes are much shorter as shown in Figure 3B. As for AZ, the decay time of the transient decreases with increasing quencher concentration, confirming that the observed transient is $BA^*(S_2)$ (see Table 2). No TG band that could be ascribed to another species was detected.

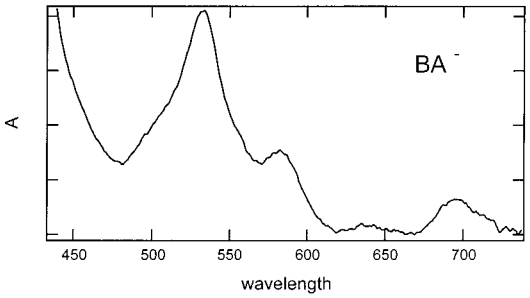

Figure 4. Steady-state absorption spectrum of $BA^{\bullet-}$ in MTHF at 77 K prepared by γ irradiation.

To our knowledge, the absorption spectrum of $BA^{\bullet-}$ has not been reported in the literature. For this reason, $BA^{\bullet-}$ has been prepared by γ-irradiation in a MTHF matrix at 77 K, and its absorption spectrum is shown in Figure 4. This spectrum somewhat overlaps with that of $BA^*(S_2)$ and therefore the presence of $BA^{\bullet-}$ during the first few picoseconds after excitation, while $BA^*(S_2)$ has not been totally quenched, might be difficult to notice. However, one can safely rule out the presence of $BA^{\bullet-}$ population with a longer lifetime than that of $BA^*(S_2)$. As the quenching efficiency at a given concentration increases with the electron donating ability of the quencher, a quenching mechanism other than CS can be safely ruled out. As for AZ, the absence of a $BA^{\bullet-}$ population can be explained by a CR occurring faster than the quenching process itself. The occurrence of a fast CR is confirmed by a negligibly small separation efficiency.

The efficiencies of the $S_2 \rightarrow T_1$ and $S_1 \rightarrow T_1$ intersystem-crossings of BA are not known but can be expected to be negligibly small, as for AZ. Therefore, the T_1 state of BA is most probably not populated. Even if it was populated, its energy is not high enough to allow ET quenching with the donors used here.

As for $AZ^{\bullet-}/D^{\bullet+}$ pairs, the very efficient CR within $BA^{\bullet-}/D^{\bullet+}$ pair can be explained by the additional reaction pathway to the excited neutral state $BA^*(S_1)$. Indeed, CR to the neutral ground state is highly exergonic and varies from about -3 to -2.27 eV with VER and DMA as donor, respectively. Therefore, CR should in principle take place in the inverted region. The free energy for CR to $BA^*(S_1) + D$ ranges from -1.35 to -0.6 eV, i.e., close to the barrierless region. The lifetime of $BA^*(S_1)$ is not known, but it can be expected to be as short as that of $AZ^*(S_1)$. This could explain why this state has not been observed after the CR of $BA^{\bullet-}/D^{\bullet+}$ pairs.

(C) $XA^{\bullet-}/D^{\bullet+}$ Pairs. Figure 5A shows a TG spectrum observed 5 ps after excitation at 400 nm of a solution of XA in ACN. As shown in Figure 5C, this bands decays exponentially with a time constant of 14 ps. The TG spectrum is very similar to the TA spectrum reported in benzene by Hochstrasser and co-workers and assigned to $XA^*(S_2)$.[46] Moreover, a S_2 fluorescence lifetime of 14 ps has been reported for XA in ACN.[47]

The S_2 lifetime of XA is known to be strongly solvent dependent: it varies from about 180 ps in perfluoro-1,3-dimethylcyclohexane[48] to 8 ps in toluene.[47] The origin of this solvent dependence is still not completely understood.[47] Contrary to the investigation of Hochstrasser et al.,[46] the long-lived transient with an absorption maximum at 550 nm and ascribed to $XA^*(T_1)$ was not observed in ACN. T_1-T_2 inversion is known to occur by going from nonpolar to polar solvents.[49] The band observed in benzene corresponds to the absorption of a (n,π^*) T_1 state, whereas the lowest triplet state in ACN has a (π,π^*) configuration.[50] In polar solvents, both triplet states

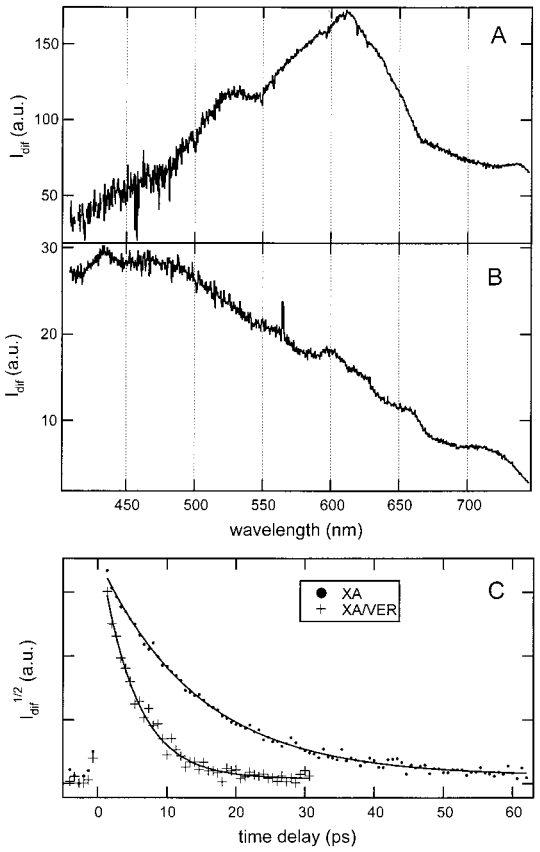

Figure 5. (A) Transient grating spectrum obtained 5 ps after excitation at 400 nm of a solution of XA in ACN; (B) transient grating spectrum obtained 20 ps after excitation at 400 nm of a solution of XA + 1 M DABCO in ACN; (C) time profile of the square root of the diffracted intensity at 615 nm measured with XA and with XA + 1 M VER in ACN.

TABLE 3: Decay Time of $XA^*(S_2)$, τ_{S2}, with Various Electron Donors in ACN

A/D	ΔG_{ET}	ΔG_{CR}	τ_{S2} (ps)
XA alone			13
XA/ANI (1 M)	−0.02	−2.88	13
XA/VER (1 M)	−0.33	−2.57	5.5
XA/DMB (1 M)	−0.44	−2.46	3.5
XA/DMA (1 M)	−1.08	−1.82	3.5
XA/DABCO (1 M)	−1.10	−1.80	5.5

are very close in energy, and thus the $^3(n,\pi^*)$ state should be thermally populated. As already stated above, the TG intensity is proportional to the square of the absorbance changes. Therefore, according to the relative intensity of the TA bands of $XA^*(S_2)$ and $XA^*(^3(n,\pi^*))$ reported by Hochstrasser et al.,[46] the maximum TG intensity due to the $XA^*(^3(n,\pi^*))$ population in ACN should be more than 7 times smaller than the initial TG intensity due to $XA^*(S_2)$. This intensity effect, together with the large width of the bands, might explain why this state was not observed in the TG spectra.

Self-quenching of the triplet state of XA has been reported to be diffusion controlled.[51] With a rate constant of diffusion of 2×10^{10} M^{-1} s^{-1} in ACN and a XA concentration of 2.5×10^{-4} M, the rate constant of self-quenching amounts to 5×10^6 s^{-1}. This process is therefore too slow to account for the nonobservation of $XA^*(^3(n,\pi^*))$ in the picosecond time scale.

Addition of a high concentration of electron donor results in a substantial decrease of the decay time of $XA^*(S_2)$ (Figure 5C), which is correlated with ΔG_{CS}, as shown in Table 3. With VER and DMB as donors, no new band was observed in the

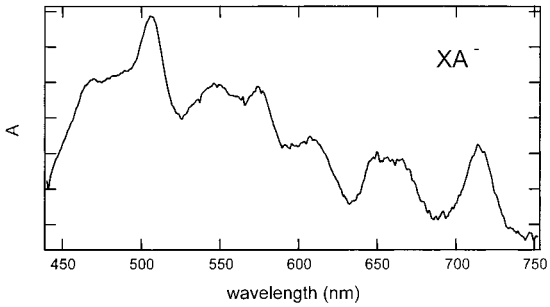

Figure 6. Steady-state absorption spectrum of $XA^{\bullet-}$ in MTHF at 77 K prepared by γ irradiation.

TABLE 4: Free Ion Yield, Φ_{ion}, Measured with XA and Strong Donors in ACN

D_s	Φ_{ion}
2×10^{-4} M DMA	0.025
0.01 M DMA	0.20
0.3 M DMA	0.24
1 M DMA	0.12
0.001 M DABCO	0.20
0.007 M DABCO	0.25
0.13 M DABCO	0.27
1 M DABCO	0.11

TG spectrum. Figure 6 shows the absorption spectrum of $XA^{\bullet-}$ formed by γ-irradiation in a MTHF matrix at 77 K. Similarly to $AZ^{\bullet-}/D^{\bullet+}$ and $BA^{\bullet-}/D^{\bullet+}$ pairs, the CR seems to be too fast for an ion population to be observed after the complete quenching of $XA^*(S_2)$. With these two donors, the separation efficiency is essentially equal to zero.

The situation is different with the stronger donors, abbreviated D_s for the remaining of this paper, DMA and DABCO. In this case, the free ion yield is clearly different from zero and depends on the quencher concentration, as shown in Table 4. First, Φ_{ion} increases with increasing D_s concentration up to 0.1 to 0.3 M. A further augmentation of the quencher concentration results in a decrease of the free ion yield. Figure 5B, shows the TG spectrum measured with the system XA/DABCO, 20 ps after excitation. The TG band due to $XA^*(S_2)$ has completely decayed, and a relatively weak and broad band can be observed. The intensity of this band remains constant over the whole time window of the TG experiment (up to 200 ps). By comparison with the spectrum shown in Figure 6, this band can be reasonably ascribed to $XA^{\bullet-}$. The absence of structure in the TG spectrum can be due first to the contribution of dispersion and second to the different experimental conditions. At short time delay, this band is hidden by that of $XA^*(S_2)$, and thus the early dynamics of $XA^{\bullet-}$ cannot be determined. The same behavior has been observed with DMA.

The concentration dependence of Φ_{ion} can be understood by considering the energy diagram shown in Figure 7. Both $XA^{\bullet-}/DMA^{\bullet+}$ and $XA^{\bullet-}/DABCO^{\bullet+}$ ion pairs states are located below $XA^*(S_1)$, and therefore DMA and DABCO can additionally quench this state. $XA^*(S_1)$ is certainly too short-lived for ET quenching to be efficient at low quencher concentration. However, $XA^*(T_1)$ is formed with a high yield and has a sufficiently long lifetime to react with an electron donor at low concentration.[51] As the resulting GIP is in a triplet state, CR is spin forbidden and the separation efficiency is essentially unity. Therefore, ET quenching of $XA^*(T_1)$ results in a large free ion yield as observed. However, if the donor concentration is large, $XA^*(S_2)$ has a high probability to be quenched. In this case, the resulting GIP is in a singlet state and CR is spin allowed. The energy of $XA^*(T_1)$ in polar solvents is not known,[49] but

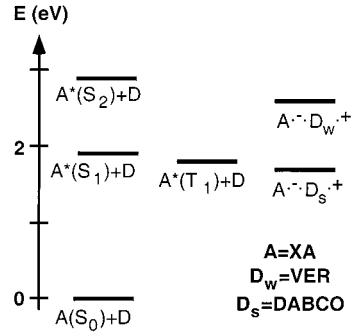

Figure 7. Energy diagram of the states involved in the photoinduced ET reaction of XA with VER and DABCO.

TABLE 5: Free Ion Yield, Φ_{ion} Measured with XA + 1 mM DABCO + 1 M Weak Donors, D_w, in ACN, $XA^*(S_2)$ Quenching Efficiency, Φ_q, and Free Ion Yield Expected in the Case of CR to the Neutral Ground State, Φ_{ion} (S_0)

D_w	Φ_q	Φ_{ion}	$\Phi_{ion}(S_0)$
ANI	0.0	0.14	
VER	0.60	0.13	0.056
DMB	0.70	0.11	0.042

these results suggest that this state must lie above the $XA^{\bullet-}/D_s^{\bullet+}$ states. The reduction potential of XA is similar to that of 9,10-dicyanoanthracene (DCA), therefore the spin-allowed CR dynamics for $XA^{\bullet-}/DMA^{\bullet+}$ should be comparable to that for $DCA^{\bullet-}/DMA^{\bullet+}$, for which a time constant of 3 ps has been measured.[26] Consequently, the spin-allowed CR of the $XA^{\bullet-}/DMA^{\bullet+}$ pair can be expected to be faster than the ET quenching of $XA^*(S_2)$. This is in agreement with the fact that the early dynamics of the TG band ascribed to $XA^{\bullet-}$ cannot be observed.

The very fast $XA^*(S_1)$-$XA^*(T_1)$ intersystem crossing[52] can be used to determine the CR pathways of GIPs formed with the weak donors (D_w: VER and DMB) and located above $XA^*(S_1)$. Indeed, if CR results in $XA^*(S_1) + D_w$, the concentration of $XA^*(T_1)$ should be unaffected by the ET quenching of $XA^*(S_2)$ (see Figure 7). On the contrary, if CR results in $XA(S_0) + D_w$, the concentration of $XA^*(T_1)$ should decrease upon ET quenching of $XA^*(S_2)$: a complete quenching of $XA^*(S_2)$ followed by CR to $XA(S_0) + D_w$, should result in a zero $XA^*(T_1)$ yield.

Instead of measuring the concentration of $XA^*(T_1)$, we have measured the ion yield of the system XA/1mM DABCO with and without a high concentration of D_w. At 1 mM, DABCO can only quench $XA^*(T_1)$, and the resulting free ion yield reflects the concentration of $XA^*(T_1)$. This procedure was used because no absorption band of $XA^*(T_1)$ could be found in ACN in the range 450−700 nm. To take into account the decrease of the dielectric constant of the sample solution upon addition of a large concentration of quencher, Φ_{ion} was first measured with the system XA/1 mM DABCO/1 M ANI. The oxidation potential of ANI is too large for this molecule to act as an ET quencher of $XA(S_2)$. Indeed, the lifetime of $XA^*(S_2)$ is unaffected by presence of 1 M ANI in ACN. The Φ_{ion} value with this reference system is 0.14. The same yield was obtained with the system XA/1 mM DABCO/1 M toluene. Table 5 shows the free ion yields obtained with the systems XA/1 mM DABCO/1 M D_w in ACN. This table also shows the free ion yield that would be expected if CR of the GIP would result in the formation of $XA(S_0) + D_w$ only. This yield is due to the fact that the $XA^*(S_2)$ population is not entirely quenched, even at 1 M D_w concentration. The unquenched $XA^*(S_2)$ populates $XA^*(T_1)$, which can then undergo ET with D_s. It can be seen that Φ_{ion}, hence the concentration of $XA^*(T_1)$, is almost

unaffected by the ET quenching of $XA^*(S_2)$. This indicates rather clearly that the main CR pathway of the GIP is that leading to the excited product $XA^*(S_1) + D_w$. The small departure from the reference value of 0.14 might be due to the effect of a high D_w concentration on the dielectric constant of the solution, the dielectric constant of D_w being not exactly the same as that of ANI or toluene, or to the fact that CR to the ground state $XA(S_0) + D_w$ state is also operative but considerably less efficient.

Concluding Remarks

Although the primary product has not been directly observed, we have presented strong evidence of the formation of an electronically excited product in a highly exergonic CR reaction. This conclusion is based on two main observations:

(i) The lifetime of a geminate ion pair is shortened by a factor of more than 50 by the presence of a lower lying electronic state of the product.

(ii) The triplet yield of XA is essentially unaffected by the ET quenching of XA in the S_2 state.

The effect of a low lying excited product state is to substantially reduce the exergonicity of CR and to shift the process from the inverted to the barrierless regime. In the present case, CR is faster than the primary CS reaction and therefore the GIP population could not be observed.

This observation strongly suggests that this could also occur for highly exergonic CS processes, when low lying excited states of the radical ions are available. The A/D systems used by Rehm and Weller to investigate highly exergonic reactions ($\Delta G_{CS} \leq -2.3$ eV) consist of tetracyanoethylene (TCNE) as electron acceptor and several aromatic hydrocarbons as electron donors (naphthalene, dimethyl-anthracene, pyrene,...).[2] The radical anion $TCNE^{\bullet -}$ is rather exceptional in that the energy of its first electronic excited state is rather high, around 2.6 eV.[33] Therefore, $TCNE^{\bullet -}*$ is certainly not generated in these highly exergonic CS reactions. On the other hand, the radical cations of all the electron donors used with TCNE have an electronic excited state below 1.6 eV and therefore CS to $TCNE^{\bullet -} + D^{\bullet +}*$ is no longer in the inverted regime. Consequently, the formation of excited radical ions in highly exergonic CS reactions might be a rather general process, as most radical ions have electronically excited states below 2 eV.

Acknowledgment. We thank Prof. E. Haselbach for supplying benz[*a*]azulene, Prof. P. Belser for the determination of the reduction potential of xanthione, and Dr. P. Bednarek for assistance in measuring the absorption spectra of the radical anions in low temperature matrixes. We also thank Mr. J. -L. Roulin for the synthesis of xanthione and the purification of many compounds. This work was supported by the Fonds national suisse de la recherche scientifique through project number 2000-055388.98.

References and Notes

(1) Marcus, R. A.; Sutin, N. *Biochim. Biophys. Acta* **1985**, *811*, 265.
(2) Rehm, D.; Weller, A. *Isr. J. Chem.* **1970**, *8*, 259.
(3) Tachiya, M.; Murata, S. *J. Phys. Chem.* **1992**, *96*, 8441.
(4) Hug, G. L.; Marciniak, B. *J. Phys. Chem.* **1995**, *99*, 1478.
(5) Haselbach, E.; Bally, T. *Pure Appl. Chem.* **1984**, *56*, 1203.
(6) Cook, A. R.; Curtiss, L. A.; Miller, J. R. *J. Am. Chem. Soc.* **1997**, *119*, 5729.
(7) Zimmer, K.; Hoppmeier, M.; Schweig, A. *Chem. Phys. Lett.* **1998**, *293*, 366.
(8) Zimmer, K.; Gödicke, B.; Hoppmeier, M.; Meyer, H.; Schweig, A. *Chem. Phys.* **1999**, *248*, 263.
(9) Ichinose, N.; Tanaka, T.; Kawanishi, S.; Suzuki, T.; Endo, K. *J. Phys. Chem. A* **1999**, *103*, 7923.
(10) Gumy, J.-C.; Vauthey, E. *J. Phys. Chem. A* **1997**, *101*, 8575.
(11) Weller, A.; Zachariasse, K. In *Chemiluminescence and Bioluminescence*; Cornier, M., Hercules, D. M., Lee, J., Eds.; Plenum Press: New York, 1973; p 169.
(12) Park, S.-M.; Tryk, D. A. *Rev. Chem. Intermed.* **1981**, *4*, 43.
(13) Haselbach, E.; Vauthey, E.; Suppan, P. *Tetrahedron* **1988**, *44*, 7335.
(14) Högemann, C.; Vauthey, E. *J. Phys. Chem. A* **1998**, *102*, 10051.
(15) Levin, P. P.; Pluzhnikov, P. F.; Kuzmin, V. A. *Chem. Phys. Lett.* **1988**, *147*, 283.
(16) Vauthey, E. In *Ultrafast Phenomena XII*; Elsaesser, T., Mukamel, S., Murnane, M. M., Scherer, N. F., Eds.; Springer: Berlin, 2000; p 485.
(17) Parker, C. A. *Photoluminescence of Solutions*; Elsevier: Amsterdam, 1968.
(18) Parker, V. D. *J. Am. Chem. Soc.* **1976**, *98*, 98.
(19) Binsch, G.; Heilbronner, E.; Jankow, R.; Schmidt, D. *Chem. Phys. Lett.* **1967**, *1*, 135.
(20) Fry, A. J.; Fox, P. C. *Tetrahedron* **1986**, *42*, 5255.
(21) Huber, J. R.; Mahaney, M. *Chem. Phys. Lett.* **1975**, *30*, 410.
(22) Siegerman, H. In *Techniques of Chemistry*; Weinberg, N. L., Ed.; John Wiley: New York, 1975; Vol. V, p 667.
(23) Gould, I. R.; Ege, D.; Moser, J. E.; Farid, S. *J. Am. Chem. Soc.* **1990**, *112*, 4290.
(24) Jacques, P.; Burget, D.; Allonas, X. *New. J. Chem.* **1996**, *20*, 933.
(25) Högemann, C.; Pauchard, M.; Vauthey, E. *Rev. Sci. Instrum.* **1996**, *67*, 3449.
(26) Vauthey, E. *J. Phys. Chem. A* **2001**, *105*, 340.
(27) Vauthey, E.; Pilloud, D.; Haselbach, E.; Suppan, P.; Jacques, P. *Chem. Phys. Lett.* **1993**, *215*, 264.
(28) von Raumer, M.; Suppan, P.; Jacques, P. *J. Photochem. Photobiol. A* **1997**, *105*, 21.
(29) Vauthey, E.; Henseler, A. *J. Photochem. Photobiol. A* **1998**, *112*, 103.
(30) Shida, T.; Haselbach, E.; Bally, T. *Acc. Chem. Res.* **1984**, *17*, 180.
(31) Mann, F. G.; Turnbull, J. H. *J. Chem. Soc.* **1951**, 757.
(32) Weller, A.; Rehm, D. *Ber. Bunsen-Ges. Phys. Chem.* **1969**, *73*, 834.
(33) Shida, T. *Electronic Absorption Spectra of Radical Ions*; Elsevier: Amsterdam, 1988; Vol. Physical Sciences data 34.
(34) Murov, S. L.; Carmichael, I.; Hug, G. L. *Handbook of Photochemistry*; Marcel Dekker: New York, 1993.
(35) Mataga, N.; Asahi, T.; Kanda, Y.; Okada, T.; Kakitani, T. *Chem. Phys.* **1988**, *127*, 249.
(36) Foggi, P.; Bussotti, L. *EPA NL* **1999**, *66*, 1.
(37) Wagner, B. D.; Szymanski, M.; Steer, R. P. *J. Phys. Chem.* **1992**, *96*, 6, 7904.
(38) Kray, H. J.; Nickel, B. *Chem. Phys.* **1980**, *53*, 235.
(39) Nickel, B.; Klemp, D. *Chem. Phys.* **1993**, *174*, 297.
(40) Vauthey, E.; Högemann, C.; Allonas, X. *J. Phys. Chem. A* **1998**, *102*, 7362.
(41) Edward, J. T. *J. Chem. Educ.* **1970**, *4*, 261.
(42) Vauthey, E. *J. Phys. Chem.* **2000**, *104*, 1804.
(43) Wurzer, A. J.; Wilhelm, T.; Piel, J.; Riedle, E. *Chem. Phys. Lett.* **1999**, *299*, 296.
(44) Högemann, C.; Vauthey, E. *Isr. J. Chem.* **1998**, *38*, 181.
(45) Yamaguchi, H.; Ninomiya, K.; Fukuda, M. *Spectrochim. Acta* **1980**, *36A*, 1003.
(46) Anderson, R. E.; Hochstrasser, R. M.; Pownall, H. J. *Chem. Phys. Lett.* **1976**, *43*, 224.
(47) Ho, C. J.; Motyka, A. L.; Topp, M. R. *Chem. Phys. Lett.* **1989**, *158*, 51.
(48) Maciejewski, A.; Steer, R. P. *J. Am. Chem. Soc.* **1983**, *105*, 6738.
(49) Maciejewski, A.; Szymanski, M.; Steer, R. P. *Chem. Phys. Lett.* **1988**, *143*, 559.
(50) Kumar, C. V.; Qin, L.; Das, P. K. *J. Chem. Soc. Far. Trans. 2* **1984**, *80*, 783.
(51) Kozlowski, J.; Maciejewski, A.; Szymanski, M.; Steer, R. P. *J. Chem. Soc., Faraday Trans.* **1992**, *88*, 557.
(52) Molenkamp, L. W.; Weitekamp, D. P.; Wiersma, D. A. *Chem. Phys. Lett.* **1983**, *99*, 382.